

DESTRIPIANDO EL ARTÍCULO:

PHYSICAL REVIEW A **69**, 062320 (2004)

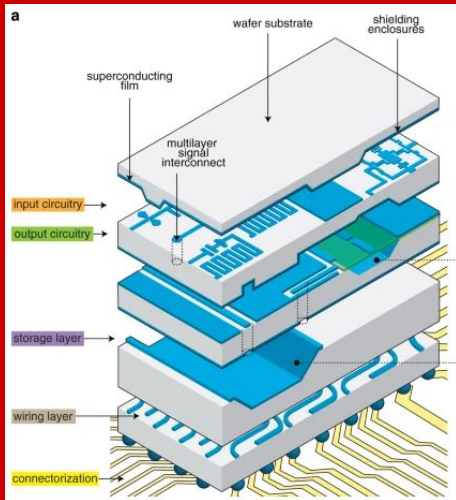
Cavity quantum electrodynamics for superconducting electrical circuits: An architecture for quantum computation

Alexandre Blais,¹ Ren-Shou Huang,^{1,2} Andreas Wallraff,¹ S. M. Girvin,¹ and R. J. Schoelkopf¹

¹*Departments of Physics and Applied Physics, Yale University, New Haven, Connecticut 06520, USA*

²*Department of Physics, Indiana University, Bloomington, Indiana 47405, USA*

(Received 7 February 2004; published 29 June 2004; corrected 23 July 2004)



Curso de Introducción a la óptica cuántica: Manipulación de átomos ultrafríos con campos electromagnéticos

Alumno: Méndez Martin; Docente: Cormick Cecilia

09.04.2022

¿De qué va el artículo?



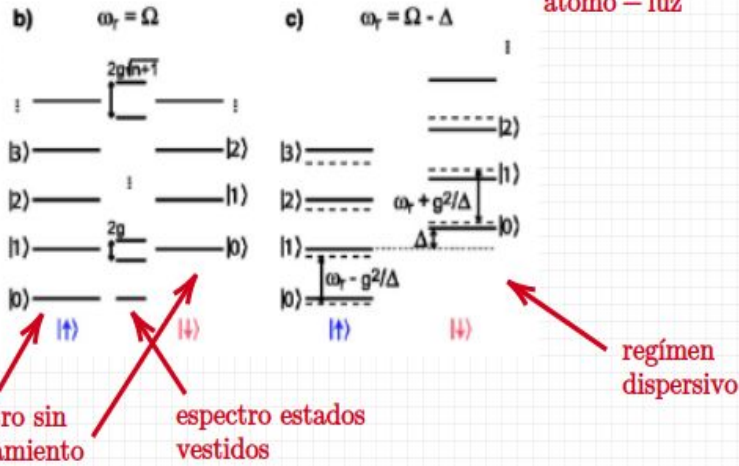
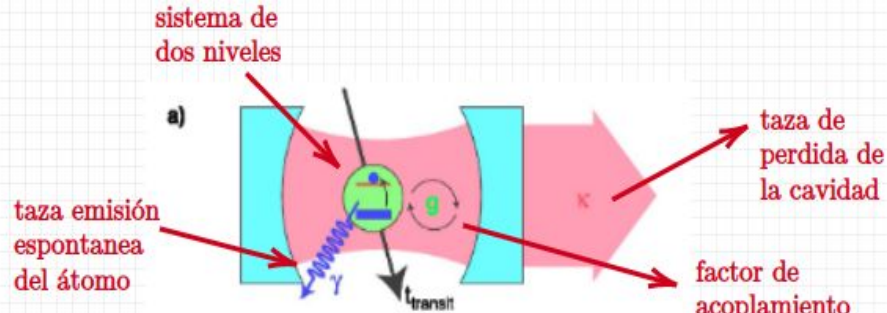
- Proponen una arquitectura para computación cuántica usando transmisiones en resonadores 1D
 - Estudian el régimen de acoplamiento fuerte entre cavidad QED y circuitos eléctricos superconductores.
 - Ofrecen una analogía macroscópica de experimentos de física atómica y permiten, potencialmente, computación y control cuántico.
 - Logran una fuerte inhibición contra la emisión espontánea.
 - Presentan potencialidad para producir entrelazamiento de múltiples qubits a tiempos largos, permitiendo mediciones de alta fidelidad.
 - Logran comunicación cuántica a través de microondas.
-

ASÍ ESTÁ ESTRUCTURADO EL ARTÍCULO

- I. **Introducción**
 - II. **Resumen Breve de una cavidad QED**
 - III. **Implementación del circuito de una cavidad QED**
 - A. Cavidad: Resonador stripline coplanar
 - B. Átomo artificial: La caja de pares de Cooper
 - C. Sistema combinado: Cavidad QED Superconductora
 - IV. **Cero detuning**
 - V. **Gran detuning: tiempo de vida de entrelazamiento**
 - VI. **Lectura QND dispersiva de qubits**
 - A. Protocolo de medición
 - B. Tiempo de medición y back action
 - C. Señal de ruido
 - VII. **Control coherente**
 - VIII. **Resonador para un bus cuántico: entrelazamiento de múltiples qubits**
 - IX. **Universalidad codificada y subespacio libre de decoherencia**
-

II. RESUMEN BREVE DE UNA CAVIDAD QED

Hamiltoniano de Jaynes-Cumming



$$\hat{H}_{JC} = \underbrace{\hbar\omega_r \left(\hat{a}^\dagger \hat{a} + \frac{1}{2} \right)}_{\text{cavidad}} + \underbrace{\frac{\hbar\Omega}{2} \hat{\sigma}^z}_{\text{átomo}} + \underbrace{\hbar g (\hat{a}^\dagger \hat{\sigma}^- + \hat{\sigma}^+ \hat{a})}_{\text{acoplamiento}} \rightarrow \left(\begin{array}{l} \text{Acoplamiento débil} \\ \text{Jaynes - Cumming model} \end{array} \right)$$

$$\left\{ |\pm, n\rangle = \cos(\theta_n) \cdot \begin{pmatrix} |\downarrow, n\rangle \\ |\uparrow, (n+1)\rangle \end{pmatrix} \pm \sin(\theta_n) \cdot \begin{pmatrix} |\uparrow, (n+1)\rangle \\ |\downarrow, n\rangle \end{pmatrix} \wedge |\uparrow, 0\rangle \right\} \rightarrow \left(\begin{array}{l} \text{estados} \\ \text{vestidos} \end{array} \right)$$

$$E_{\pm, n} = (n+1)\hbar\omega_r \pm \frac{\hbar}{2} \sqrt{4g^2(n+1) + \Delta^2} \rightarrow \left(\begin{array}{l} \text{auto} \\ \text{energías} \end{array} \right)$$

$$\Delta \stackrel{\text{def}}{=} (\Omega - \omega_r) \rightarrow \text{(detuning)}; \theta_n = \frac{1}{2} \arctan\left(\frac{2g\sqrt{n+1}}{\Delta}\right)$$

$$g/\Delta \ll 1 \Rightarrow \left\{ \begin{array}{l} \left\{ |\pm, n\rangle \approx \begin{pmatrix} |\downarrow, 0\rangle \\ |\uparrow, 1\rangle \end{pmatrix} \pm \left(\frac{g}{\Delta}\right) \cdot \begin{pmatrix} |\uparrow, 1\rangle \\ |\downarrow, 0\rangle \end{pmatrix} \right\} \rightarrow \left(\begin{array}{l} \text{auto} \\ \text{estados} \end{array} \right) \\ \left\{ \Gamma_{\pm, 0} \approx \begin{pmatrix} \gamma \\ \kappa \end{pmatrix} + \left(\frac{g}{\Delta}\right) \cdot \begin{pmatrix} \kappa \\ \gamma \end{pmatrix} \right\} \rightarrow \left(\begin{array}{l} \text{taza de} \\ \text{decaimiento} \end{array} \right) \end{array} \right.$$

$$\hat{H}_{\text{eff}} = \hbar \left[\underbrace{\omega_r + \frac{g^2}{\Delta} \hat{\sigma}^z}_{\text{ac Stark shift}} \right] \hat{a}^\dagger \hat{a} + \frac{\hbar}{2} \left[\underbrace{\Omega + \frac{g^2}{\Delta}}_{\text{Lamb shift}} \right] \hat{\sigma}^z \rightarrow \left(\begin{array}{l} \text{régimen} \\ \text{dispersivo} \end{array} \right)$$



III. IMPLEMENTACIÓN DE CIRCUITO DE UNA CAVIDAD QED

A. Cavity: Resonador stripline coplanar

Conceptos a refrescar

- Circuito RLC
- Factor Q



Conceptos nuevos

- Stripline



Paper...

Circuito LC

$Q \sim 10^6$ ($Q \sim 10^4$)

Técnica litográfica (CQED)

B. Átomo artificial: La caja de pares de Cooper

Conceptos a refrescar

- Juntura Josephson
- Pares de Cooper



Conceptos nuevos

- Trasmones
- Caja de pares de Cooper
- Qubits de carga

Paper...

Hamiltoniano



C. Sistema combinado: Cavity QED Superconductora

Paper...

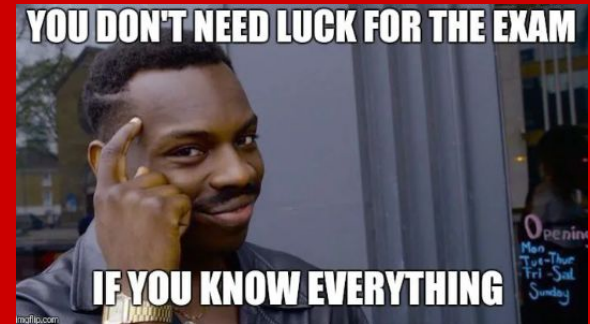
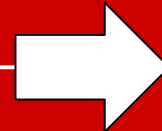
Hamiltoniano

Mapeo Hamiltoniano JC



Paper...

The on-chip of CQED



IV. CERO DETUNING

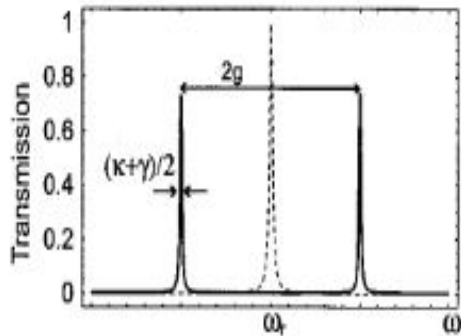
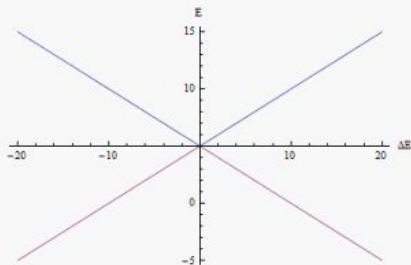


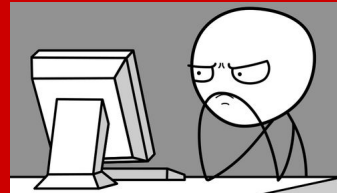
FIG. 4. Expected transmission spectrum of the resonator in the absence (dashed line) and presence (solid line) of a superconducting qubit biased at its degeneracy point. Parameters are those presented in Table I. The splitting exceeds the line width by two orders of magnitude.



Recordar el avoided crossing



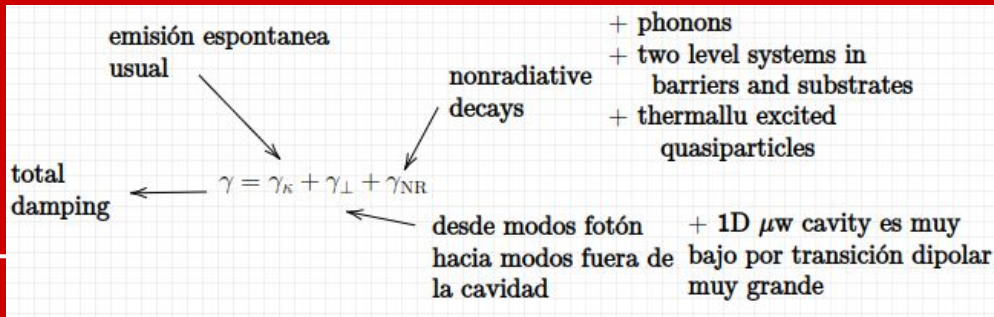
V. GRAN DETUNING: TIEMPO DE VIDA DE ENTRELAZAMIENTO



Qubit fuera de la cavidad: el ruido se acopla directamente al qubit y produce transiciones, al aplicar una fuente.

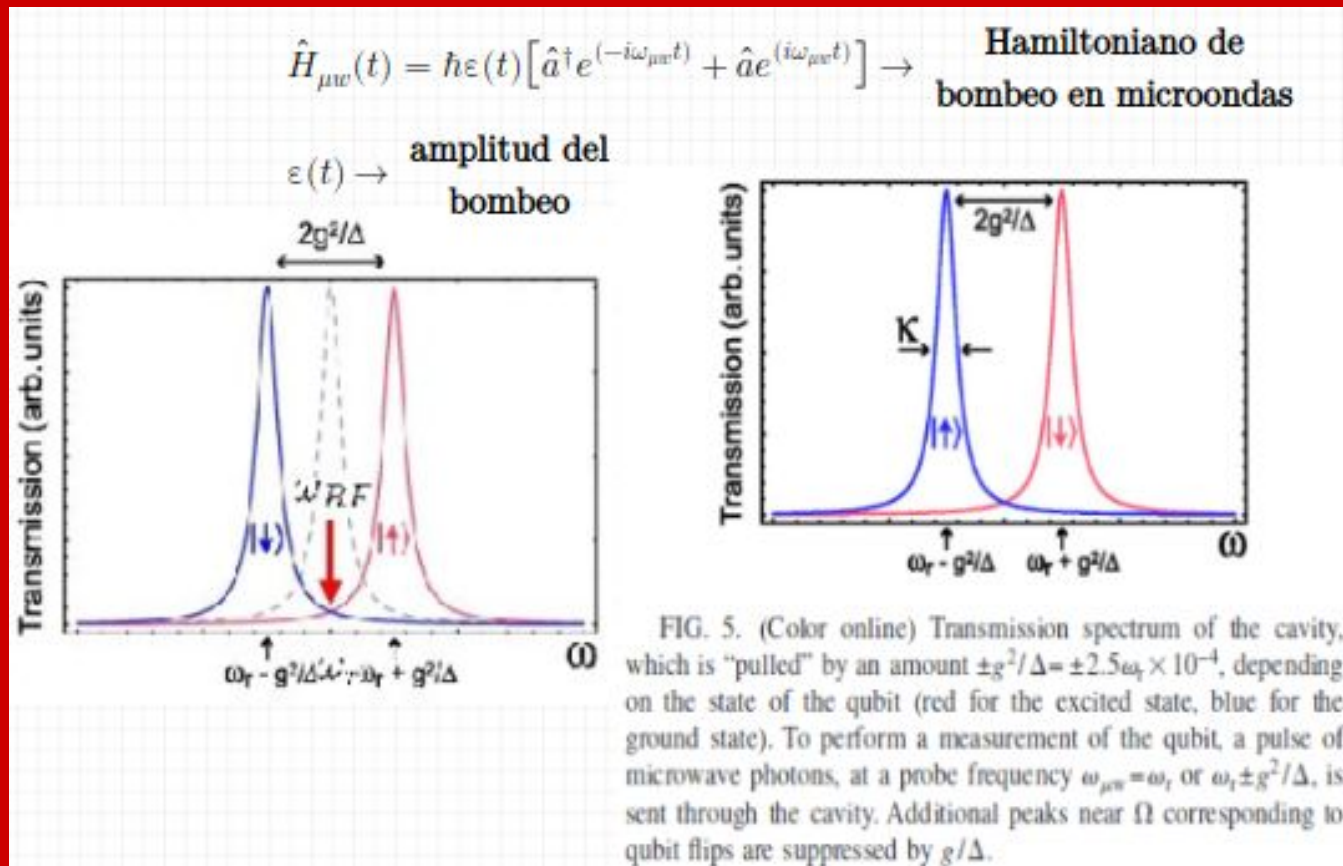
Qubit dentro de la cavidad: el ruido no se acopla directamente y se reduce notablemente la parte real de la impedancia del ambiente.

$$T_l \approx \mathcal{O}(1\mu s) \rightarrow \left(\begin{array}{c} \text{qubit not} \\ \text{inside cavity} \end{array} \right); T_l \approx \mathcal{O}(64\mu s) \rightarrow \left(\begin{array}{c} \text{qubit} \\ \text{inside cavity} \end{array} \right)$$



VI. LECTURA QND DISPERSIVA DE QUBITS

A. PROTOCOLO DE MEDICIÓN

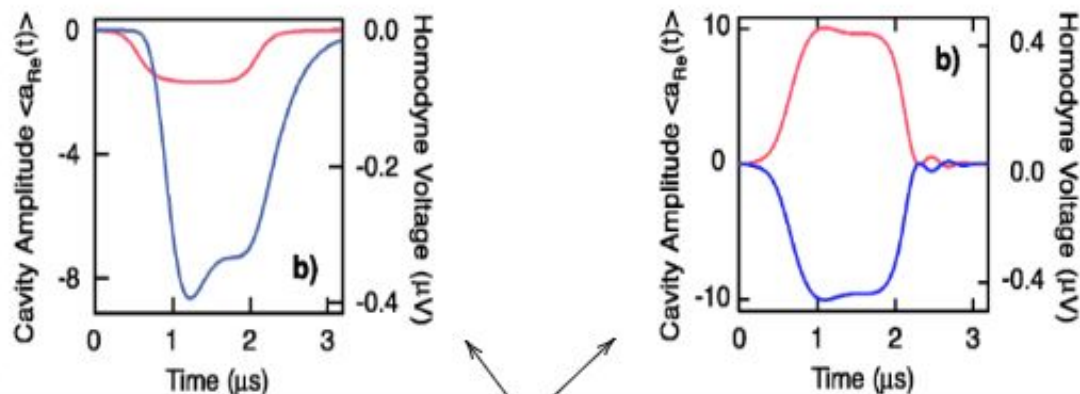
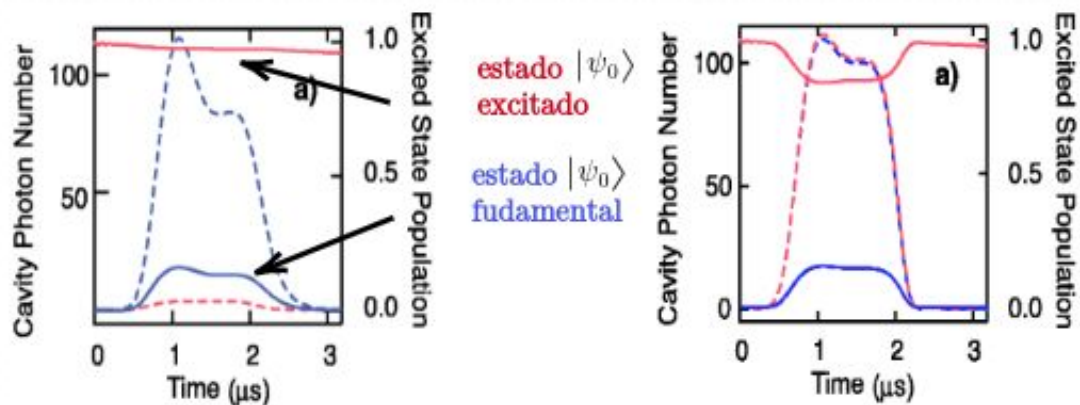


VI. LECTURA QND DISPERSIVA DE QUBITS

A. PROTOCOLO DE MEDICIÓN

En realidad son dos propuestas

Resultados de métodos numéricos



CASO I

$$\omega_{\mu w} = w_r + g^2/\Delta$$

marco rotante
con $\omega_{\mu w}$

CASO II

$$\omega_{\mu w} = w_r$$

VI. LECTURA QND DISPERSIVA DE QUBITS

A. Tiempo de medición y back action

$$\hat{H}_{\text{eff}} = \hbar[\omega_r + \underbrace{\frac{g^2}{\Delta} \hat{\sigma}_z}_{\text{ac Stark shift}}] \hat{a}^\dagger \hat{a} + \frac{\hbar}{2} \left[\Omega + \underbrace{\frac{g^2}{\Delta}}_{\text{Lamb shift}} \right] \hat{\sigma}_z \rightarrow \left(\begin{array}{l} \text{régimen} \\ \text{dispersivo} \end{array} \right)$$

- Desfase del qubit induce tiempo de desfase, debe ser \ll tiempo de medición.
- Microondas induce transiciones entre estados de un qubit.

$$\text{SNR} = \frac{P_{\text{signal}}}{P_{\text{noise}}} \rightarrow \text{Signal to noise ratio}$$

B. Señal de ruido

TABLE II. Figures of merit for readout and multiqubit entanglement of superconducting qubits using dispersive (off-resonant) coupling to a 1D transmission-line resonator. The same parameters as Table I and a detuning of the Cooper-pair box from the resonator of 10% ($\Delta=0.1\omega_r$) are assumed. Quantities involving the qubit decay γ are computed both for the theoretical lower bound $\gamma=\gamma_\kappa$ for spontaneous emission via the cavity and (in parentheses) for the current experimental upper bound $1/\gamma \geq 2 \mu\text{s}$. Though the signal to noise of the readout is very high in either case, the estimate of the readout error rate is dominated by the probability of qubit relaxation during the measurement, which has a duration of a few cavity lifetimes [$\sim(1-10)\kappa^{-1}$]. If the qubit nonradiative decay is low, both high-efficiency readout and more than 10^3 two-bit operations could be attained.

Parameter	Symbol	1D circuit
Dimensionless cavity pull	$g^2/\kappa\Delta$	2.5
Cavity-enhanced lifetime	$\gamma_\kappa^{-1}=(\Delta/g)^2\kappa^{-1}$	64 μs
Readout SNR	$\text{SNR}=(n_{\text{cni}}/n_{\text{amp}})\kappa/2\gamma$	200 (6)
Readout error	$P_{\text{err}}\sim 5\times\gamma/\kappa$	1.5% (14%)
One-bit operation time	$T_\pi>1/\Delta$	>0.16 ns
Entanglement time	$t_{\sqrt{\text{SWAP}}}=\pi\Delta/4g^2$	$\sim 0.05 \mu\text{s}$
Two-bit operations	$N_{\text{op}}=1/[\gamma t_{\sqrt{\text{SWAP}}}]$	>1200(40)

VII. CONTROL COHERENTE

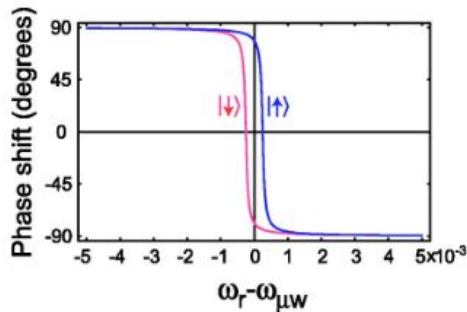


FIG. 8. (Color online) Phase shift of the cavity field for the two states of the qubit as a function of detuning between the driving and resonator frequencies. Obtained from the steady-state solution of the equation of motion for $a(t)$ while only taking into account damping on the cavity and using the parameters of Table I. Readout of the qubit is realized at, or close to, zero detuning between the drive and resonator frequencies where the dependence of the phase shift on the qubit state is largest. Coherent manipulations of the qubit are realized close to the qubit frequency which is 10% detuned from the cavity (not shown on this scale). At such large detunings, there is little dependence of the phase shift on the qubit's state.

$$H_{1q} = \frac{\hbar}{2} \left[\Omega + 2\frac{g^2}{\Delta} \left(a^\dagger a + \frac{1}{2} \right) - \omega_{\mu w} \right] \sigma^z + \hbar \frac{g\epsilon(t)}{\Delta} \sigma^x + \hbar(\omega_r - \omega_{\mu w}) a^\dagger a + \hbar\epsilon(t)(a^\dagger + a)$$

$$\omega_{\mu w} = \left(\Omega + (2n + 1) \frac{g^2}{\Delta} \right) \Rightarrow \text{rot. } x \text{ with } \omega = \frac{g\epsilon}{\Delta}$$

$$\omega_{\mu w} = \left(\Omega + (2n + 1) \frac{g^2}{\Delta} - \frac{2g\epsilon}{\Delta} \right) \Rightarrow \text{Hadamard transf}$$

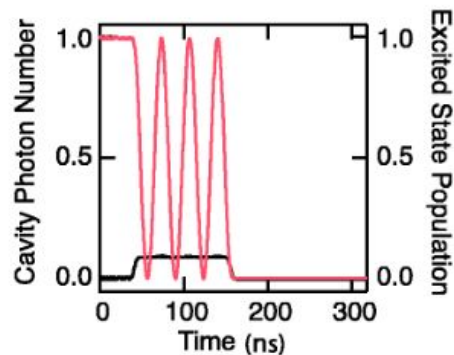
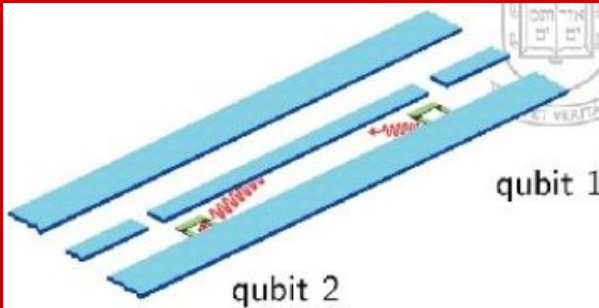


FIG. 9. (Color online) Numerical stochastic wave function simulation showing coherent control of a qubit by microwave irradiation of the cavity at the ac Stark- and Lamb-shifted qubit frequency. The qubit (red line) is first left to evolve freely for about 40 ns. The drive is turned on for $t=7\pi\Delta/2g\epsilon \sim 115$ ns, corresponding to 7π pulses, and then turned off. Since the drive is tuned far away from the cavity, the cavity photon number (black line) is small even for the moderately large drive amplitude $\epsilon=0.03 \omega_r$ used here.

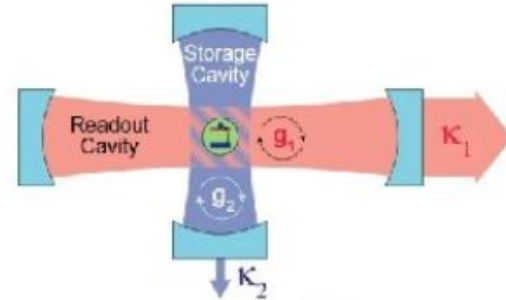
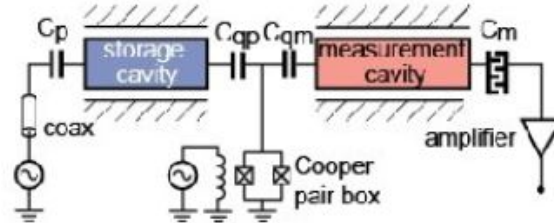
Ya terminamos... sólo unos comentarios más!

VIII. RESONADOR PARA UN BUS CUÁNTICO: ENTRELAZAMIENTO DE MÚLTIPLES QUBITS

IX. UNIVERSALIDAD CODIFICADA Y SUBESPACIO LIBRE DE DECOHERENCIA



High-Q cavity as quantum memory



$$H_{2q}^{\text{eff}} \approx \hbar \left[\omega_r + \underbrace{\frac{g^2}{\Delta} (\sigma_i^z + \sigma_j^z)}_{\text{Stark shifts}} \right] a^\dagger a + \frac{1}{2} \hbar \left[\Omega + \underbrace{\frac{g^2}{\Delta}}_{\text{Lamb shifts}} \right] (\sigma_i^z + \sigma_j^z) + \underbrace{\hbar \frac{g^2}{\Delta} (\sigma_i^+ \sigma_j^- + \sigma_i^- \sigma_j^+)}_{\text{acople a través de excitaciones virtuales de el resonador}}$$

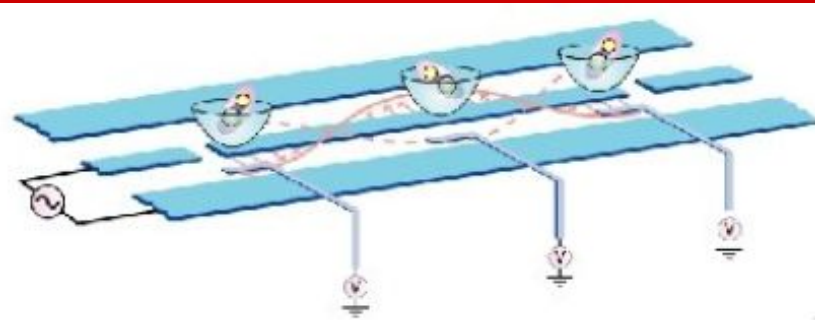
$$U_{2q}(t) = \exp \left[-i \frac{g^2}{\Delta} t \left(a^\dagger a + \frac{1}{2} \right) (\sigma_i^z + \sigma_j^z) \right] \otimes \begin{pmatrix} 1 & & & \\ & \cos\left(\frac{g^2}{\Delta} t\right) & i \sin\left(\frac{g^2}{\Delta} t\right) & \\ & i \sin\left(\frac{g^2}{\Delta} t\right) & \cos\left(\frac{g^2}{\Delta} t\right) & \\ & & & 1 \end{pmatrix} \otimes \hat{I}_r$$

marco rotante

CNOT gate
√iSWAP gate

⇒ universal quantum computation

in resonator space



Ya terminamos... solo unos comentarios más!

LEY DE MOORE CUÁNTICA?!!

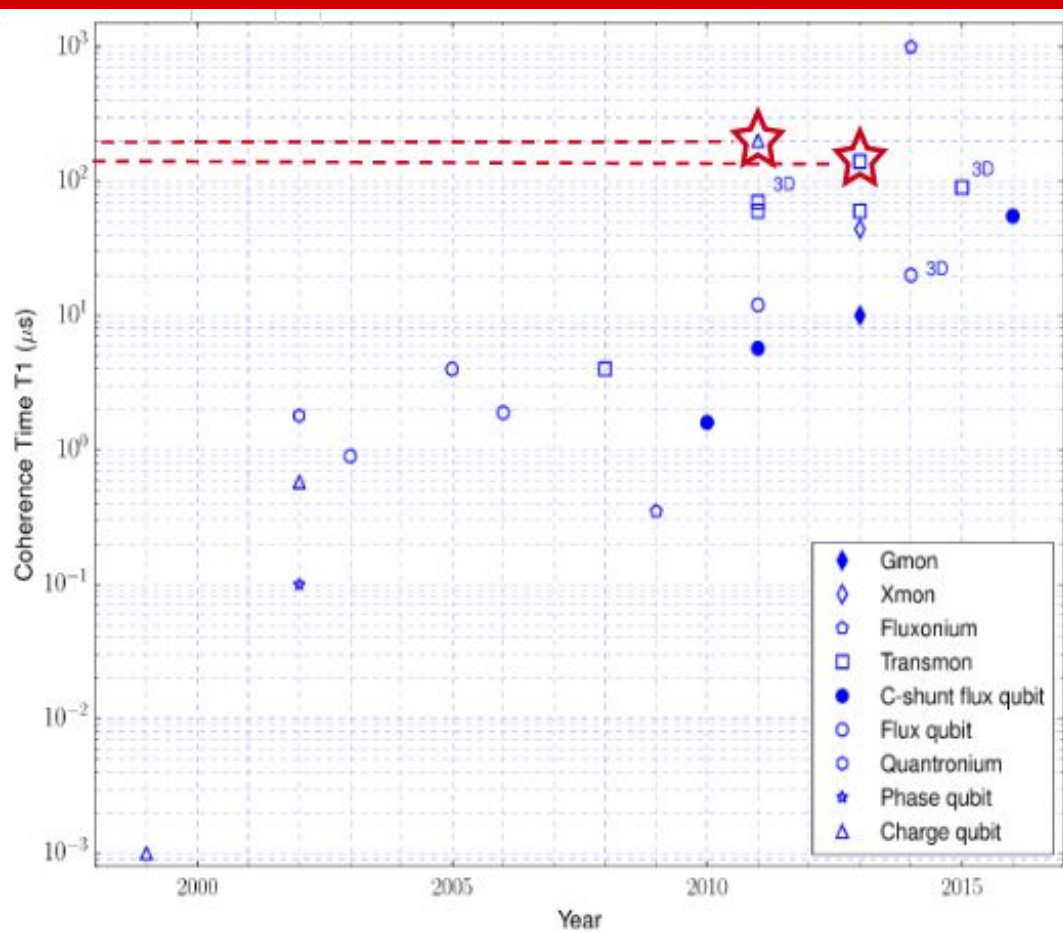


Fig. 32. Similar to the famous Moore's law for semiconductor industry, the coherence times of superconducting qubits also appear to exhibit exponential scaling. The graph shows, on a logarithmic scale, the energy-relaxation time T_1 achieved through the years in some state-of-the-art superconducting qubits. T_1 has increased by six orders of magnitude since 1999. This remarkable progress has been driven by novel circuit design, material and fabrication improvements [23], and understanding of dissipation mechanisms [61,1214].

Ya terminamos... solo unos comentarios más!

Table 1

Comparison between natural atoms and artificial atoms based on superconducting circuits and their interaction with quantized bosonic modes.

	Natural atoms		Artificial atoms
	Neutral atoms	Trapped ions	Superconducting qubits
Qubits	Atoms	Ions	Josephson-junction devices
Dimensions	$\sim 10^{-10}$ m	$\sim 10^{-10}$ m	$\sim 10^{-6}$ m
Energy gap	$\sim 10^{14}$ Hz (optical), GHz (hyperfine)	$\sim 10^{14}$ Hz (optical), GHz (hyperfine)	$\sim 1-10$ GHz
Quantized bosonic modes	Photons	Collective vibration modes of ions (phonons)	LC circuits (photons), surface acoustic waves (phonons)
Frequency range	Microwave, optical	Microwave, optical	Microwave
Controls	Lasers	Lasers, electric/magnetic fields	Microwave pulses, voltages, currents
Components	Mirrors Optical and microwave cavities Optical fibers Beam-splitters	Electrodes Optical cavities, vibration modes Optical fibers Beam-splitters	Capacitors LC and transmission-line resonators, 3D cavities Transmission lines Hybrid couplers, Josephson mixers
Temperature	nK- μ K	μ K-mK	~ 10 mK
Advantages	Homogeneous (parameters set by nature)	Long coherence times	Strong and controllable coupling, tunable in situ, fabricated on chip

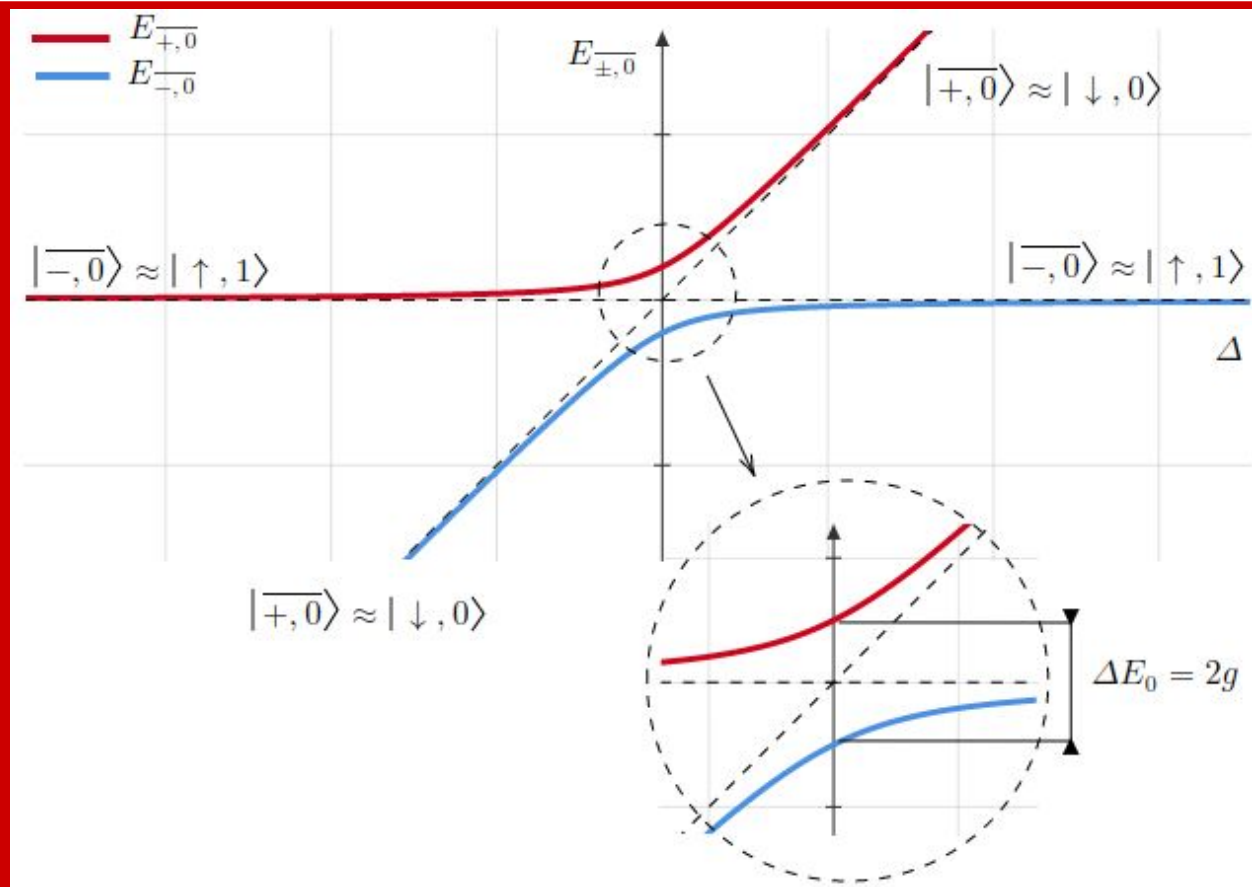
¡Muchas gracias!



II. Resumen breve de una cavidad QED

Hamiltoniano de Jaynes-Cumming

Recordando el
Avoided Crossing...



III. Implementación del circuito de una cavidad QED

Recordemos las propiedades del Circuito RLC clásico y el factor Q

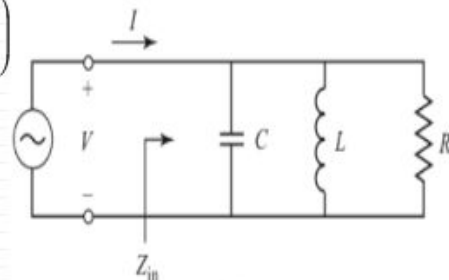
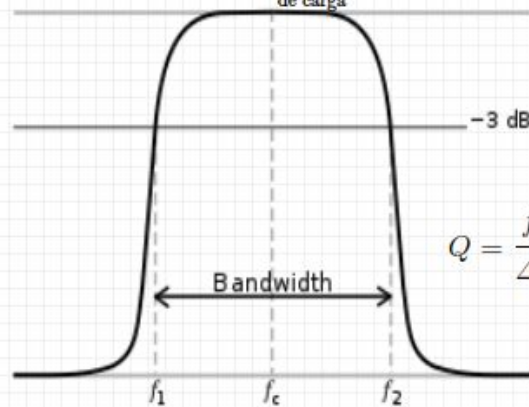
$$(Z_{in})^{-1} = [R^{-1} + (j\omega L)^{-1} + (j\omega C)^{-1}] \rightarrow (\text{impedancia}); \omega_0 = \frac{1}{\sqrt{LC}} \rightarrow \left(\begin{array}{l} \text{frecuencia de} \\ \text{resonancia} \end{array} \right)$$

$$W_E = \frac{1}{2} |V|^2 C \rightarrow \left(\begin{array}{l} \text{energía eléctrica} \\ \text{almacenada} \end{array} \right) \quad W_B = \frac{1}{2} I^2 L \rightarrow \left(\begin{array}{l} \text{energía magnética} \\ \text{almacenada} \end{array} \right)$$

$$P_{in} = \frac{1}{2} V I^* \rightarrow \left(\begin{array}{l} \text{potencia de} \\ \text{entrada} \end{array} \right); P_{loss} = \frac{|V|^2}{2R} \rightarrow \left(\begin{array}{l} \text{potencia} \\ \text{discipada} \end{array} \right)$$

$$Q_{int} = \frac{\omega(W_E + W_B)}{P_{loss}} \rightarrow \left(\begin{array}{l} \text{factor de} \\ \text{calidad} \end{array} \right) \Rightarrow Q_{int} = \frac{R}{\omega_0 L} = \omega_0 R C \rightarrow \left(\begin{array}{l} \text{factor de calidad} \\ \text{en resonancia} \end{array} \right)$$

$$(Q_{tot})^{-1} = \left[\underbrace{\left(\begin{array}{l} \text{circuito} \\ \text{interno} \end{array} \right)^{-1}}_{\text{efectos de carga}} + \underbrace{\left(\begin{array}{l} \text{circuito} \\ \text{externo} \end{array} \right)^{-1}}_{\text{efectos de carga}} \right] \rightarrow \left(\begin{array}{l} \text{factor de} \\ \text{calidad total} \end{array} \right)$$



$$Q = \frac{f_0}{\Delta f} \rightarrow \left(\begin{array}{l} \text{factor de} \\ \text{calidad} \end{array} \right)$$

$$\tau = Q/2f \rightarrow \left(\begin{array}{l} \text{tiempo de vida} \\ \text{de 1 fotón} \end{array} \right)$$

A mayor Q mayor nitidez de la frecuencia de resonancia...



III. Implementación del circuito de una cavidad QED

¿Qué es un stripline?!

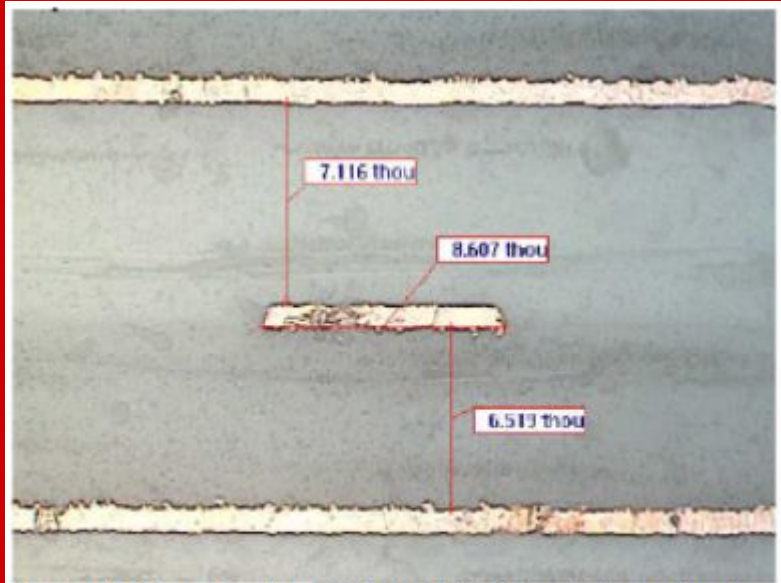


Figure 4: Cross Section of Typical Stripline to Show Conductor Roughness. The label "thou" Represents Thousandths of an Inch.

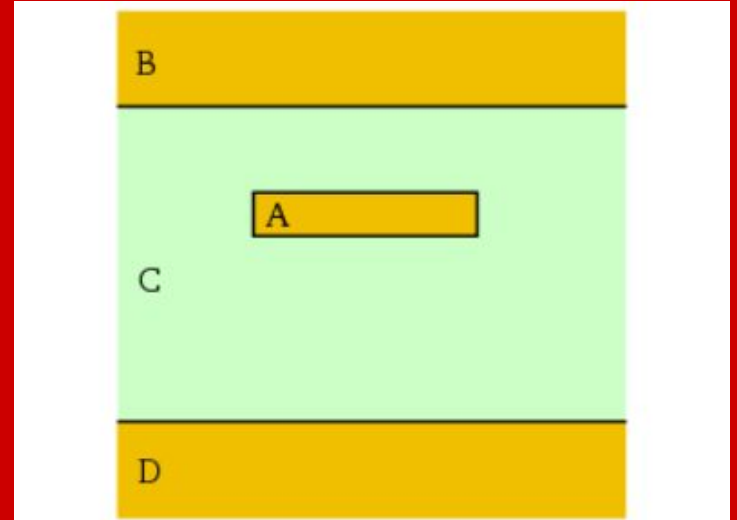


Figure 2: Diagrama de la sección transversal de la geometría de una línea stripline. El conductor central (A) se inserta entre las líneas de tierra (B y D). La estructura está soportada por un dieléctrico (C).



III. Implementación del circuito de una cavidad QED

- ¿Junta Josephson?
- ¿Pares de Cooper?
- ¿Qubit de carga?
- ¿Transmones?

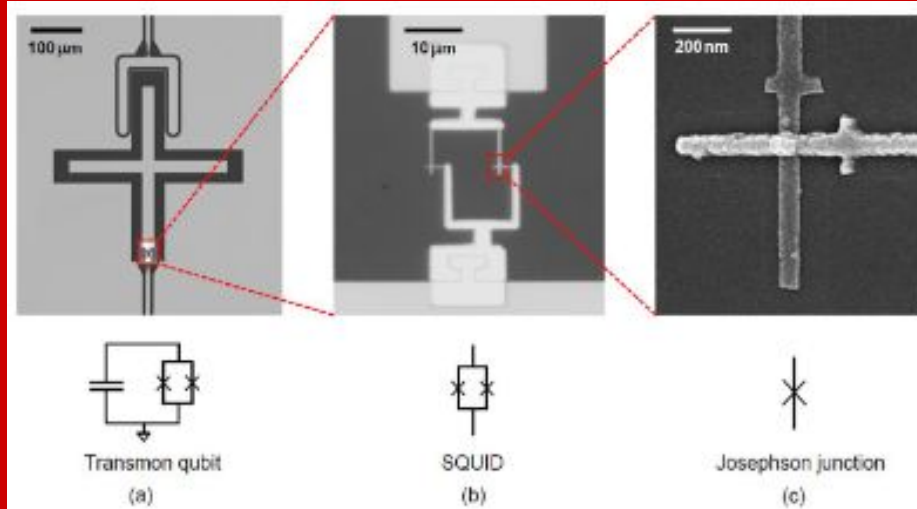
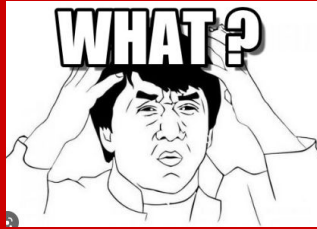


Fig. 6: Images of a frequency tunable transmon qubit. (a) The entire transmon consisting of a large capacitance (the “+” shape) in parallel with a SQUID to ground. A zoom in of the SQUID and a single Josephson junction are in (b) and (c), respectively.

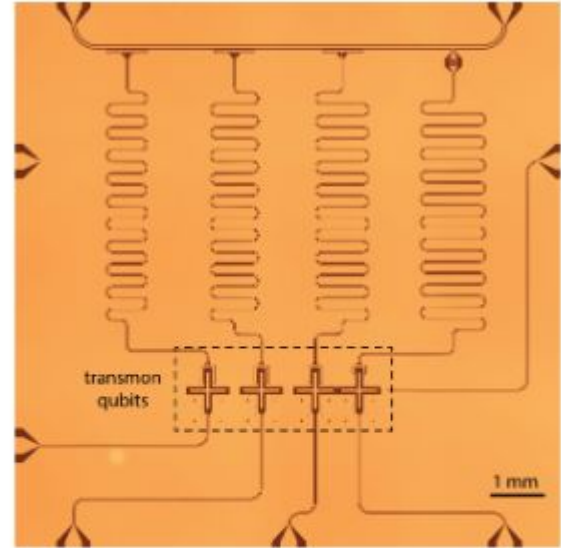


Fig. 1: Optical image of a typical circuit QED device with four transmon qubits and the accompanying on-chip microwave network needed to operate the device. Each arm of the transmons are $\sim 300 \mu\text{m}$ long and form a $\sim 70 \text{ fF}$ capacitance to ground. The main operating frequencies of the transmons in this device are around 5 GHz, but this can be tuned *in situ* between approximately 4 to 6 GHz. The surrounding microwave transmission lines are used to control the transmons and monitor their quantum states through microwave spectroscopy.



III. Implementación del circuito de una cavidad QED

¿Por qué es necesaria la juntura de Josephson?

ii Anarmonicidad!!
Fundamental para lograr la computación cuántica.

Se prende E_J y comienza el tuneo, la degeneración desaparece y se abren los gaps!!

Sistema periódico, nos concentramos en vecindad de degeneración

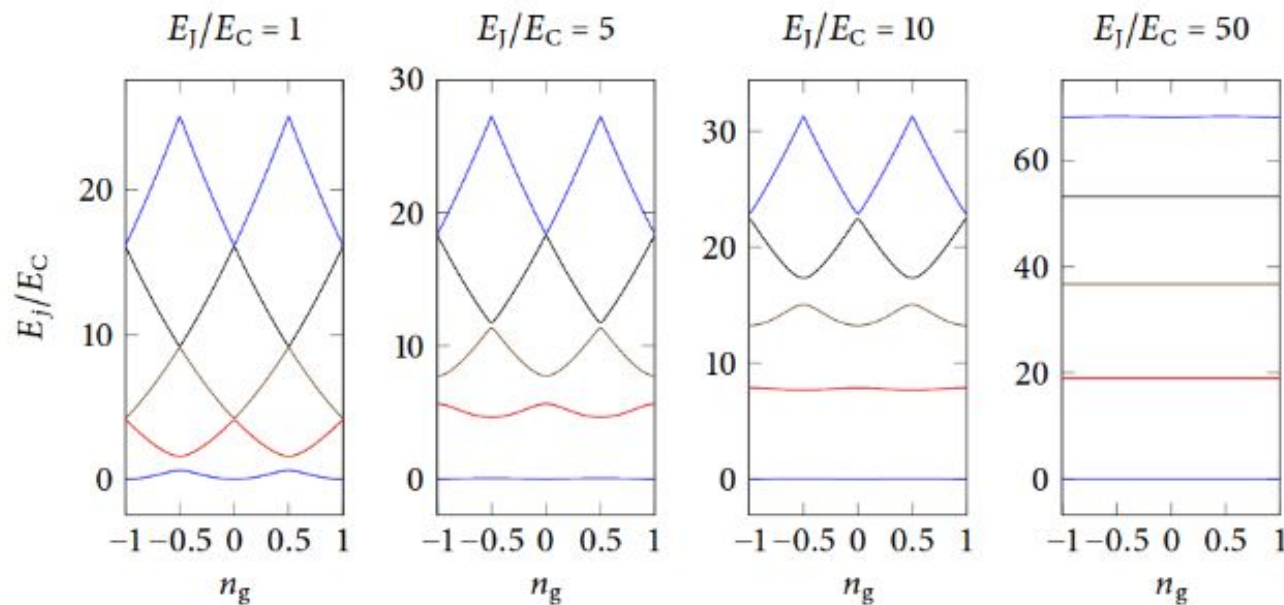
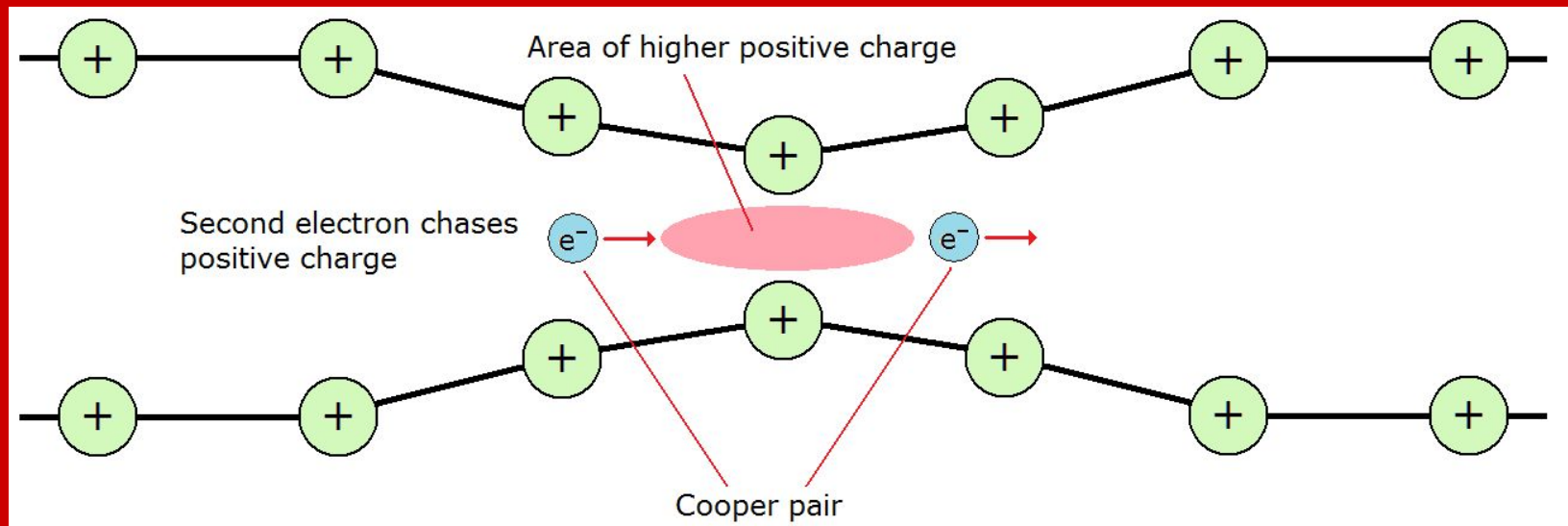


Figure 2.5: Charge dispersion. The energies of the lowest 5 levels of the transmon Hamiltonian (2.30), in units of the charging energy E_C . For low E_J/E_C ratio, the energies are parabolic functions of the offset charge n_g , with avoided crossings; as the ratio is increased the levels become exponentially flatter.

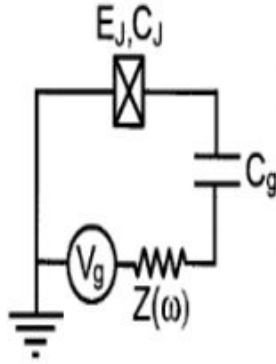
III. Implementación del circuito de una cavidad QED

¿Qué son los pares de Cooper?



III. Implementación del circuito de una cavidad QED

$$\hat{H}_Q = \underbrace{4E_c \sum_N (N - N_g)^2 |N\rangle \langle N|}_{\text{Energía de Carga}} - \underbrace{\frac{E_J}{2} \sum_N (|N+1\rangle \langle N| + \text{H. c.})}_{\text{Energía de Josephson}}$$



$E_c = e^2/2C_\Sigma \rightarrow$ (energía de carga)

$C_\Sigma = (C_J + C_g) \rightarrow$ (capacitancia total)

$C_g \rightarrow$ (capacitancia de la isla)

$E_J \rightarrow$ (energía de acoplamiento de Josephson)

$N_g = C_g V_g / 2e \rightarrow$ (brecha de energía normalizada)

$N \in \mathbb{N} \rightarrow$ (número de pares de Cooper)

$E_c \gg E_J \Rightarrow \hat{H}_Q = -\frac{E_{el}}{2} \hat{\sigma}^z - \frac{E_J}{2} \hat{\sigma}^x \rightarrow$ (Hamiltoniano)

$E_{el} = 4E_C(1 - 2N_g) \rightarrow$ (régimen de carga) (¿Por qué?)

Paper...

Cooper-pair box

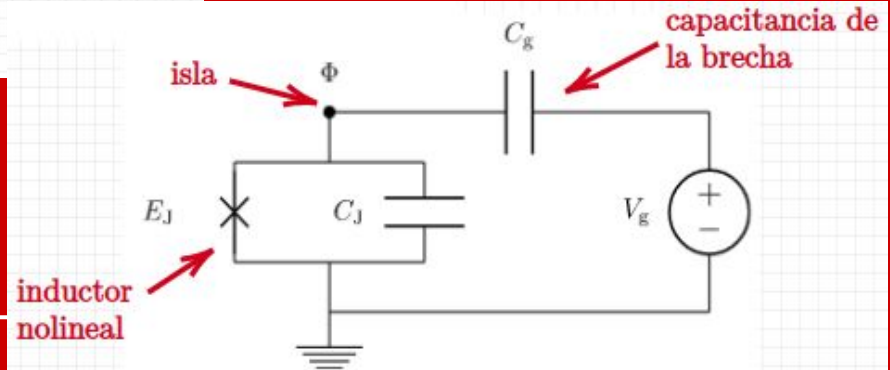
Se puede mapear una partícula con pseudospin-1/2 con campos efectivos en x y en z.

Las energías escalan cuadráticamente con N_g entonces el régimen de carga permite medir y manipular bien los qubits.

Y más...

FIG. 3. Circuit diagram of the Cooper-pair box. The gate voltage is connected to the island through an environmental impedance $Z(\omega)$.

¿Charge qubit? Son estados que representan la presencia o ausencia de exceso de pares de Cooper en la isla. La superposición de estados de carga pueden manipularse con voltaje V_g de la juntura.



III. Implementación del circuito de una cavidad QED

Hamiltoniano de la cavidad QED superconductor

$$\hat{H}_Q = \overbrace{-2E_c(1 - 2N_g^{dc})\bar{\sigma}^z - \frac{E_J}{2}\bar{\sigma}^x}_{V_g^{dc} \Rightarrow N_g \rightarrow N_g^{dc}} - e \overbrace{\frac{C_g}{C_\Sigma} \sqrt{\frac{\hbar\omega_c}{Lc}}(a^\dagger + a)}_{v=V_{rms}^0(a^\dagger+a)} \otimes (1 - 2N_g - \bar{\sigma}^z)$$

subespacio de interés

$$\text{si } \mathcal{B} = \{|\uparrow\rangle, |\downarrow\rangle\}; \theta = \arctan\left[\frac{E_J}{4E_c(1 - N_g^{dc})}\right]; \Omega = \frac{1}{\hbar}\sqrt{(E_J)^2 + [4E_c(1 - 2N_g^{dc})]^2}$$

$$\Rightarrow \tilde{H} = \left\{ \hbar\omega_r \left(a^\dagger a + \frac{1}{2} \right) + \frac{\hbar\Omega}{2} \sigma^z - e \frac{C_g}{C_\Sigma} \sqrt{\frac{\hbar\omega_r}{Lc}} (a^\dagger + a) \otimes [1 - 2N_g - \cos(\theta)\sigma^z + \sin(\theta)\sigma^x] \right\}$$

punto de degeneración de carga

$$\text{si } N_g^{dc} = \frac{C_g V_g^{dc}}{2e} = \frac{1}{2} \wedge \theta = \frac{\pi}{2}; \Omega = \frac{E_J}{\hbar}; g = -\frac{\beta|e|}{\hbar} \sqrt{\frac{\hbar\omega_r}{cL}}; \beta = \frac{C_g}{C_\Sigma}$$

Acoplamiento fuerte → modelo de Rabi

$$\Rightarrow \tilde{H}_{JC} = \left\{ \hbar\omega_r \left(a^\dagger a + \frac{1}{2} \right) + \frac{\hbar\Omega}{2} \sigma^z + \hbar g (a^\dagger + a) \sigma^x \right\} \stackrel{?}{=} \hat{H}_{JC}$$

$$\hat{H}_{JC} = \hbar\omega_r \left(\hat{a}^\dagger \hat{a} + \frac{1}{2} \right) + \frac{\hbar\Omega}{2} \hat{\sigma}^z + \hbar g (\hat{a}^\dagger \hat{\sigma}^- + \sigma^+ \hat{a})$$

Acoplamiento débil → modelo de Jaynes-Cumming

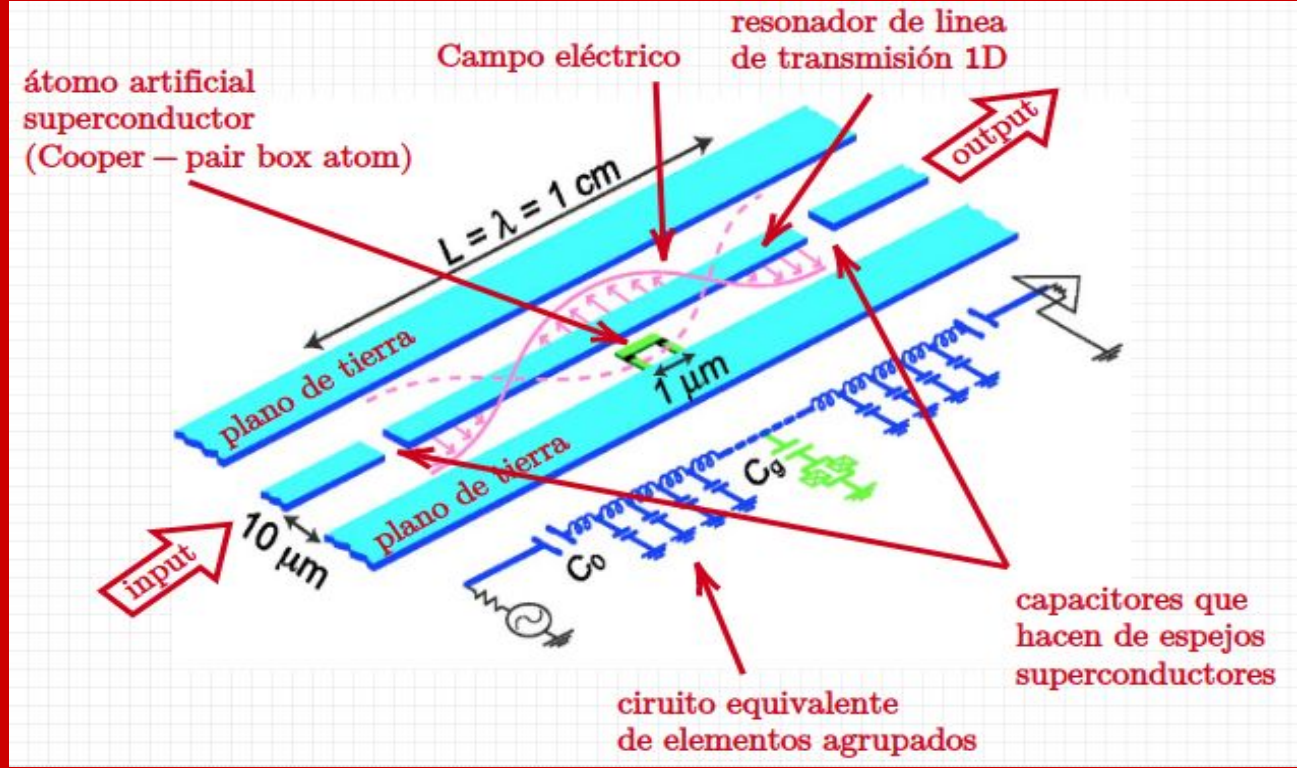
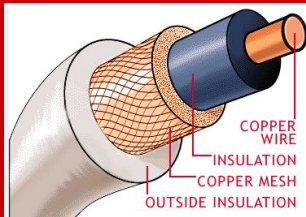
Reemplazar directamente valores particulares y sale...



III. Implementación del circuito de una cavidad QED

¿Qué es un stripline?

Analogía con cable coaxial...



VI. LECTURA QND DISPERSIVA DE QUBITS

A. Protocolo de medición

A C++ library using quantum trajectories to solve quantum master equations

Rüdiger Schack^{a,b,1}, Todd A. Brun^{b,2}

^a Department of Mathematics, Royal Holloway, University of London, Egham, Surrey TW20 0EX, UK

^b Department of Physics, Queen Mary and Westfield College, University of London, London E1 4NS, UK

Received 25 July 1996; revised 17 January 1997

$$\dot{\hat{\rho}}_{tot} = -\frac{i}{\hbar}[(\hat{H}_{sys} + \hat{H}_{\kappa} + \hat{H}_{\gamma}), \hat{\rho}_{tot}] \rightarrow \text{Ecuación de von Neuman}$$

$$\left(\begin{array}{l} \text{acople débil entre} \\ \text{modos de (cavidad} \\ \text{+qubit) y baño} \end{array} \right) \Rightarrow \dot{\hat{\rho}}_{tot} = -\frac{i}{\hbar}[\hat{H}_{sys}, \hat{\rho}_{tot}] - \dots$$

$$\dots - \frac{1}{2} \sum_{m=\{\kappa, \gamma\}} (\hat{L}_m^\dagger \hat{L}_m \hat{\rho} + \hat{\rho} \hat{L}_m^\dagger \hat{L}_m - 2\hat{L}_m \hat{\rho} \hat{L}_m^\dagger)$$

$$\hat{L}_{\kappa} = \sqrt{\kappa} \hat{a}; L_{\gamma} = \sqrt{\gamma} \hat{\sigma}^{-} \rightarrow \left(\begin{array}{l} \text{operadores} \\ \text{de Lindblad} \end{array} \right)$$

$$|d\psi\rangle = \underbrace{-\frac{i}{\hbar} \hat{H} |\psi\rangle dt + \sum_j (\hat{L}_j - \langle \hat{L}_j \rangle_{\psi}) |\psi\rangle d\xi_j + \dots}_{\text{fluctuaciones random}} + \underbrace{\dots + \sum_j \left(\langle \hat{L}_j^\dagger \rangle_{\psi} \hat{L}_j - \frac{1}{2} \hat{L}_j^\dagger \hat{L}_j - \frac{1}{2} \langle \hat{L}_j^\dagger \rangle_{\psi} \langle \hat{L}_j \rangle_{\psi} \right) |\psi\rangle dt}_{\text{drift determinista}}$$

quantum state
diffusion

$$|d\psi\rangle = \underbrace{-\frac{i}{\hbar} \hat{H} |\psi\rangle dt + \sum_j \left(\frac{\hat{L}_j}{\sqrt{\langle \hat{L}_j^\dagger \hat{L}_j \rangle_{\psi}}} - 1 \right) |\psi\rangle dN_j + \dots}_{\text{drift determinista}} + \underbrace{\dots + \sum_j \left(\frac{1}{2} \langle \hat{L}_j^\dagger \hat{L}_j \rangle_{\psi} - \frac{1}{2} \hat{L}_j^\dagger \hat{L}_j \right) |\psi\rangle dt}_{\text{fluctuaciones random}}$$

quantum
jump

$$|d\psi\rangle = \underbrace{-\frac{i}{\hbar} \hat{H} |\psi\rangle dt + \sum_j \left(\frac{\hat{L}_j - \langle \hat{L}_j \rangle_{\psi}}{\sqrt{\langle \hat{L}_j^\dagger \hat{L}_j \rangle_{\psi} - \langle \hat{L}_j^\dagger \rangle_{\psi} \langle \hat{L}_j \rangle_{\psi}}} - 1 \right) |\psi\rangle dN_j + \dots}_{\text{drift determinista}} + \underbrace{\dots + \sum_j \left(\langle \hat{L}_j^\dagger \rangle_{\psi} \hat{L}_j - \frac{1}{2} \hat{L}_j^\dagger \hat{L}_j + \frac{1}{2} \langle \hat{L}_j^\dagger \hat{L}_j \rangle_{\psi} - \langle \hat{L}_j^\dagger \rangle_{\psi} \langle \hat{L}_j \rangle_{\psi} \right) |\psi\rangle dt}_{\text{fluctuaciones random}}$$

orthogonal
jump

$$\text{procesos de Wiener independientes y complejos} \Rightarrow \begin{cases} \overline{d\xi_m} = \overline{d\xi_m d\xi_n} = 0 \\ \overline{d\xi_m^* d\xi_n} = \delta_{mn} dt \end{cases} \rightarrow \text{promedio en ensamble}$$

